

Investigation of Lattice Dynamics of Bi-Doped Strontium Bismuth Niobate Ferroelectric Ceramic

Rajveer Singh¹, Vandna Luthra², Archana³ and R.P. Tandon⁴

^{1,4}Department of Physics and Astrophysics, University of Delhi, Delhi-110007

^{2,3}Department of Physics, Gargi College, University of Delhi, Siri Fort Road, New Delhi-110049

E-mail: ¹rajveersingh@arsd.du.ac.in, ²vandna_arora@yahoo.com,

³archana851@gmail.com, ⁴ram_tandon@hotmail.com

Abstract—Polycrystalline ceramics $Sr_{1-x}Bi_{2+2x/3}Nb_2O_9$ (SBN), with x lying in the range 0.0- 0.2 were prepared by solid state reaction method. The X-ray diffraction pattern derived from the resulting data at the room temperature subjected to Rietveld analysis confirmed the formation of single phase with orthorhombic crystal structure. Raman spectroscopy was used to understand the lattice dynamics of Bi doped SBN. Observed SEM micrograph showed a uniform distribution of grains on the surface of the samples. The dielectric studies of the compounds reveals that the value of dielectric constant and transition temperature increases with increasing the Bi-content in SBN. The dielectric loss reduces significantly with bismuth addition in SBN. The dielectric diffusivity was found to increase with increase in Bi content.

1. INTRODUCTION

Bismuth layer structured ferroelectric ceramics (BLSFs) have great attention because of their potential applications in non-volatile random access memory (NVRAM) [1-3]. The best material for memory application was chosen Lead Zirconium Titanate (PZT), but one of the problems with PZT is its fatigue resistance [4]. BLSF ceramics such as $SrBi_2Nb_2O_9$ (SBN), $SrBi_2Ta_2O_9$ (SBT) and their solid solutions have much attention because of their good fatigue resistance [5, 6].

ABN ($m=2$) belongs to the family of Aurivillius compound with a general formula of $(Bi_2O_2)^{2+}(A_{m-1}B_mO_{3m+1})^{2-}$, where A and B are 12-fold and 6-fold coordinated cations respectively, in which the lattice structure is composed of m -number of $(A_{m-1}B_mO_{3m+1})^{2-}$ unit cells sandwiched between $(Bi_2O_2)^{2+}$ slabs along pseudo-tetragonal axis [7].

Ferroelectric ABN crystallizes in $A2_1am$ space group (no. 36- C_{2v}^{12}). The primitive cell contains two formula units and the structure is shown in fig. 1. Substitution or doping of any cations at any site A, Bi or Nb in these types of Aurivillius oxides modifies the crystal structure and its properties according to symmetry and valence ionic radii. Hence, many studies were done by incorporating different cations at various positions in these complexes. In this paper, an attempt is also made to study the variation of Sr/Bi ratio at A site by solving it for Raman phonons with normal coordinate analysis. Group

theoretical analysis provides the total number of 84 zone center modes as $22A_1+20A_2+20B_1+22B_2$. Out of these modes 3 modes are acoustical ($1A_1+1B_1+1B_2$) and rest of 81 modes are optical. Further $21A_1$, $19B_1$ and $21B_2$ are infrared active while all the 81 modes are Raman active ($21+20+19+21=81$). In this paper, an effort is also made to assign these phonons to their respective optical phonon modes with the investigation of the potential energy distribution to determine the significance of contribution from each force constant toward Raman wavenumbers [8, 9].

We also studied the effect of Bi doping on dielectric properties of SBN.

2. EXPERIMENTAL DETAILS

$SrCO_3$ (purity 99.99%, Sigma Aldrich), Bi_2O_3 (99.9%, CDH) and Nb_2O_5 (99.99% Sigma Aldrich) powders were used for synthesis of polycrystalline ceramics $Sr_{1-x}Bi_{2+2x/3}Nb_2O_9$ with $x=0.0, 0.1$ and 0.2 . The powders were ball milled for 24 hours in acetone medium with Zirconia balls. The resultant powders were ground for 2 hours and then calcined at $800^\circ C$ for 4 hours in conventional furnace. The PVA was mixed to calcined powder and then shaped into pellets of 10 mm diameter and 1.5 thicknesses using uniaxial Hydraulic pressure. The pellets of SBN ceramics were sintered at $1100^\circ C$ in conventional furnace with holding time of 3 hours. The specimens of $Sr_{1-x}Bi_{2+2x/3}Nb_2O_9$ with $x=0.0, 0.1$ and 0.2 are represented as SBN0, SBN1 and SBN2 respectively.

The sintered pellets were characterized by powder X-ray diffraction (Rigaku Miniflex II, with $Cu K\alpha_1$), Raman spectroscopy (Renishaw InVia Reflex Micro-Raman spectrometer) and Field effect scanning electron microscopy-FESEM (Tescan Mira 3) for their structural characterization. For electrical measurement silver paste was used as electrode and then fired at $500^\circ C$ for 30 min.

The dielectric measurements were taken as a function of temperature from room temperature to $500^\circ C$ in the frequency

range 20 Hz- 1MHz using impedance analyzer (Wayne Kerr-6500B).

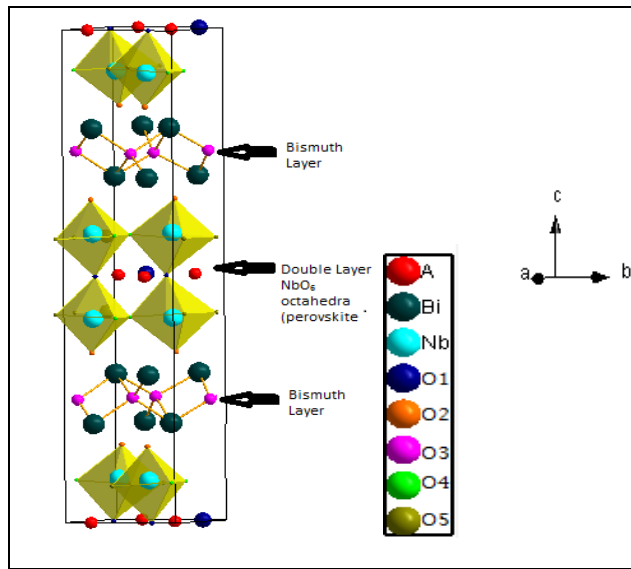


Fig. 1: Structure of distorted $\text{SrBi}_2\text{Nb}_2\text{O}_9$ showing the tilting NbO_6 octahedra along the c -axis

3. RESULTS AND DISCUSSION

Fig. 2 shows the XRD patterns of sintered pellet of SBBN ceramics for $x=0.0, 0.1$ and 0.2 . A single phase was observed in all specimens without any secondary phase with orthorhombic structure. The peaks were well defined and matched with JCPDS card no. 96-1190. The peaks were found to be shifted towards the higher angle with increasing bismuth content in SBN. The lattice constants were calculated using the Rietveld refinement and are listed in table 1. The lattice constants were found to decrease with increase Bi- content in SBN.

Table 1: The lattice parameters obtained from Reitveld refinement.

| Sample code | a (Å) | b (Å) | c (Å) | V (Å) ³ | γ |
|-------------|--------|--------|---------|--------------------|------|
| SBN0 | 5.5092 | 5.5128 | 25.0928 | 762.096 | 1.61 |
| SBN1 | 5.5088 | 5.5023 | 25.0435 | 759.095 | 1.57 |
| SBN2 | 5.5080 | 5.5095 | 25.0412 | 759.908 | 1.41 |

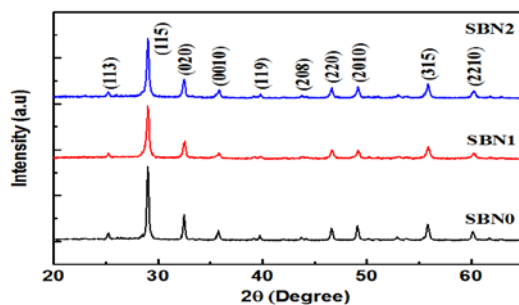


Fig. 2: XRD patterns of sintered pellets for SBN0, SBN1, and SBN2.

Fig. 2 shows the SEM micrographs of surface of sintered pellets. It can be seen from the micrographs that the SBN0 has porous structure and SBN2 has more dense structure as compared to both SBN0 and SBN1. The grain size was found to decrease with increasing Bi- content in SBN. All the micrographs have clear grain boundary.

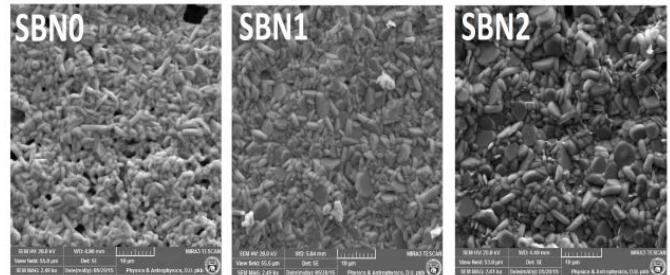


Fig. 3: SEM micrographs of sintered pellets for SBN0, SBN1, and SBN2.

Fig. 4 shows the Raman spectrum for SBN0, SBN1, and SBN2 recorded at room temperature.

The present normal coordinate analysis is based on the Wilson–GF matrix method and makes use of Cartesian symmetry coordinates [4]. The eigenvalue equation is given by

$$|FG - E\lambda| = 0$$

Where F is a matrix of force constants and thus brings the potential energies of vibrations into the equation, G is a matrix that involves the masses and certain spatial relationships of the atoms and thus brings the kinetic energies into the equation, E is a unit matrix and λ brings the frequency ν into the equation is defined by $\lambda = 4\pi^2c^2\nu^2$. The matrix F was constructed by using short range force constant model (SRFCM). The short range forces are the forces that are effective up to certain neighbors only. Their magnitude diminishes generally after the second-neighbor interatomic interactions. The stretching forces between two atoms were assumed to be obeying Hooke’s law. The stretching forces alone are not adequate to account for transverse vibrations in the lattice and therefore bending forces were included in the calculation. Potential energies include short range valence forces between nearest neighbors Nb-O2, Nb-O5, Nb-O4, Nb-O1, Bi-O3, Bi-O2, A-O1, A-O4, A-O5 and bending forces between O4-Nb-O4, O4-Nb-O5, O4-Nb-O5, O1-Nb-O1, O3-Bi-O3, Nb-O2-Bi, Nb-O2-Bi, A-O1-A and O2-Bi-O2 only where A is $\text{Sr}_{1-x}\text{Bi}_x$ ($x=0-0.2$). The input parameters used for the calculation are the lattice parameter, mass of the atoms, symmetry coordinates and the Raman wavenumbers. The short-range force constant is optimized to give the best fit of the observed Raman wavenumbers.

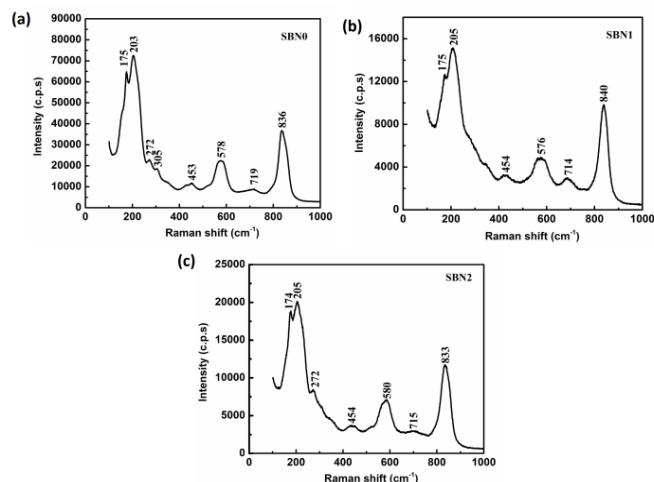


Fig. 4: Raman spectrum for (a) SBN0; (b) SBN1, and (c) SBN2.

The calculated Raman and Infrared frequencies at the zone center for SBN are given in Table 2 along with the measured values of the Raman. The present calculations with eighteen short-range force constants provide a very good agreement with the experimental values for Raman wavenumbers.

The potential energy distributions (PED) are also investigated for each normal mode in SBN. From PED, contributions of different force constants to various frequencies are determined. (The details of PED are with the author and can be made available on request.)

The highest frequencies 849.1 cm^{-1} of A1 mode, 819.0 cm^{-1} of A2 mode, 848.7 cm^{-1} of B1 mode and 819.0 cm^{-1} of B2 mode are led by vibrations of oxygen ions (O4,O5) in Nb-O plane, represented by O4-Nb-O5 force constant (These frequencies are for SBN and likewise with others). This result is in confirmation with the inferences drawn in case of SBT (Strontium Bismuth Tantalate). In comparison of SBT, these frequencies of SBN are shifted towards high frequencies which are due to lower mass of niobium [9].

Theoretically calculated result has also provided a new frequency of 736 cm^{-1} in A2 mode and 736.5 cm^{-1} in B2 mode which was not present in Bismuth Tantalate family.

According to these calculations, frequencies near 700 cm^{-1} in all the modes which corresponds well with our experimental results nano crystallites of SBN are dominated by Sr-O1 and Sr-O1-Sr force constant. In frequencies near 600 cm^{-1} , O-Nb-O chain plays an important role and found to be primarily responsible. Result of these calculations also establishes that the frequencies of 572.7 cm^{-1} in A1 mode and 571.1 cm^{-1} in B2 mode are ruled by A-O1 bond while Bi-O3 and O3-Bi-O3 bonds dominates the frequencies of 564.6 cm^{-1} in A2 mode and 564.0 cm^{-1} in B1 mode.

From theoretical calculations, Nb-O2 was found to be significant force constant for frequencies 531.4 cm^{-1} in A1 mode, 530.7 cm^{-1} in A2 mode, 531.8 cm^{-1} in B1 mode and

530.3 cm^{-1} in B2 mode. Calculations also provides frequencies of 475.1 cm^{-1} , 416.5 cm^{-1} , 381.4 cm^{-1} in A1 mode, 429.3 cm^{-1} , 416.7 cm^{-1} in A2 mode, 414.2 cm^{-1} , 400.4 cm^{-1} in B1 mode and 472.0 cm^{-1} , 429.8 cm^{-1} , 418.1 cm^{-1} in B2 mode where Bi-O3 force constant is the main contributor. In these frequencies, there is no contribution from Nb and A atoms. In other words, these frequencies are completely dominated by Bi-O3 force constant.

PED shows that the lower frequencies (50-100 cm^{-1}) are mainly contributed by vibrations of Bi atoms and most of the higher frequencies by vibrations of Bi layer and NbO₆ octahedra. This result is in confirmation with same family compound SBT [9].

The present calculations do provide a frequency near 30 cm^{-1} , in confirmation with the softening modes. Also in A1, A2 and B2 modes, another lower frequency than 28 cm^{-1} is predicted by these calculations, which needs precise experimental verifications.

Table 2: Calculated and observed wave numbers (in cm^{-1})

| Species | wave-numbers (in cm^{-1}) for SBN0 | | wave numbers (in cm^{-1}) for SBN1 | | wave numbers (in cm^{-1}) for SBN2 | |
|---------|--|-----------|--|-----------|--|----------|
| | Calculate d | Observe d | Calculate d | Observe d | Calculate d | Observed |
| A 1 | 849.1 | 836 | 857.3 | 840 | 851.2 | 833 |
| | 712 | 719 | 711.1 | 714 | 713.5 | 715 |
| | 708.6 | - | 706.5 | - | 711.2 | - |
| | 601.7 | - | 595.9 | - | 596.1 | - |
| | 572.7 | 578 | 570.2 | 576 | 570.3 | 580 |
| | 531.4 | - | 523.4 | - | 538.5 | - |
| | 475.1 | 453 | 479.6 | 454 | 476.7 | 454 |
| | 416.5 | - | 422.3 | - | 416.4 | - |
| | 381.4 | - | 386.6 | - | 381.2 | - |
| | 324.7 | 305 | 321.9 | - | 323.2 | - |
| | 275.5 | 272 | 275.9 | - | 275.8 | 272 |
| | 198.9 | 203 | 195.8 | 205 | 196.8 | 205 |
| | 196.2 | - | 193.7 | - | 192.1 | - |
| | 175 | 175 | 179.8 | 175 | 174 | 174 |
| | 147.2 | - | 146.4 | - | 144.6 | - |
| | 124.8 | - | 127.1 | - | 125.3 | - |
| | 111.8 | - | 111.3 | - | 110.2 | - |
| 96.6 | - | 99.9 | - | 97.4 | - | |
| 77.7 | - | 90.1 | - | 82.5 | - | |
| 37.6 | - | 36.7 | - | 36.6 | - | |
| 19 | - | 26.1 | - | 21.9 | - | |
| A 2 | 819 | 836 | 824.7 | 840 | 820.3 | 833 |
| | 736 | 719 | 733.2 | 714 | 736.6 | 715 |
| | 611.7 | - | 605.1 | - | 604.6 | - |
| | 564.6 | 578 | 565.9 | 576 | 569.9 | 580 |
| | 530.7 | - | 522 | - | 537.4 | - |
| | 429.3 | 453 | 435.3 | 454 | 429.2 | 454 |
| | 416.7 | - | 416.2 | - | 421.7 | - |
| | 402.9 | - | 408.3 | - | 402.8 | - |
| | 304.5 | 305 | 307.6 | - | 301.2 | - |

| | | | | | | |
|------------|-------|-------|-------|-------|-------|-----|
| | 281.4 | - | 277.2 | - | 284.7 | - |
| | 265.1 | 272 | 262.7 | - | 267 | 272 |
| | 198.3 | 203 | 206.3 | 205 | 197.7 | 205 |
| | 170.1 | 175 | 173.5 | 175 | 174.3 | 174 |
| | 125 | - | 133.2 | - | 130.3 | - |
| | 107.1 | - | 107.3 | - | 107.6 | - |
| | 97.6 | - | 97.3 | - | 91.5 | - |
| | 64.7 | - | 65.3 | - | 64.3 | - |
| | 34.8 | - | 39 | - | 37 | - |
| | 16.1 | - | 21 | - | 18 | - |
| | 6.9 | - | 11.8 | - | 10.1 | - |
| B 1 | 848.7 | 836 | 857 | 840 | 850.9 | 833 |
| | 711.9 | 719 | 711 | 714 | 713.3 | 715 |
| | 601.7 | - | 595.9 | - | 596 | - |
| | 564 | 578 | 565.4 | 576 | 569.3 | 580 |
| | 531.8 | - | 523.8 | - | 538.9 | - |
| | 414.2 | 453 | 419.9 | 454 | 414 | 454 |
| | 400.4 | - | 405.8 | - | 400.4 | - |
| | 321.5 | - | 319.2 | - | 320.3 | - |
| | 304.5 | 305 | 307.7 | - | 301 | - |
| | 276 | 272 | 276.5 | - | 276.3 | 272 |
| | 199.6 | 203 | 199.2 | 205 | 200.6 | 205 |
| | 198 | - | 196.7 | - | 194.7 | - |
| | 157.4 | - | 162.6 | - | 161 | - |
| | 114.8 | - | 118.8 | - | 115.2 | - |
| | 112.4 | - | 113 | - | 113.6 | - |
| 97.4 | - | 110.1 | - | 104.5 | - | |
| 82.4 | - | 85.3 | - | 83.1 | - | |
| 55.6 | - | 56.5 | - | 55.5 | - | |
| 34.7 | - | 38.1 | - | 35.9 | - | |
| B 2 | 819 | 836 | 824.6 | 540 | 820.3 | 833 |
| | 736.5 | - | 733.6 | - | 737.1 | - |
| | 709 | 719 | 706.9 | 714 | 711.6 | 715 |
| | 611.8 | - | 605.1 | - | 604.6 | - |
| | 571.1 | 578 | 568.8 | 576 | 569 | 580 |
| | 530.3 | - | 521.6 | - | 537.1 | - |
| | 472 | - | 476.5 | - | 473.5 | - |
| | 429.8 | 453 | 435.7 | 454 | 429.6 | 454 |
| | 418.1 | - | 417.4 | - | 423.1 | - |
| | 365.9 | - | 371 | - | 365.8 | - |
| | 282.6 | 305 | 278.7 | - | 286.5 | - |
| | 266.7 | 272 | 264.2 | - | 268.4 | 272 |
| | 199.3 | 203 | 206.7 | 205 | 198.4 | 205 |
| | 192.4 | - | 186.2 | - | 184.1 | - |
| | 161.9 | 175 | 169.6 | 175 | 163.8 | 174 |
| 127.9 | - | 131.3 | - | 129.1 | - | |
| 114.6 | - | 117.8 | - | 116.2 | - | |
| 108.8 | - | 107.9 | - | 104.7 | - | |
| 92.1 | - | 90.1 | - | 88.7 | - | |
| 48.2 | - | 47.7 | - | 46.6 | - | |
| 18.8 | - | 18.5 | - | 18.4 | - | |

The temperature dependence of dielectric constant at 1 kHz is shown in the Fig. 4. The dielectric constant was calculated using the formula $\epsilon'_r = C/C_0$, where C_0 is the geometrical capacitance and C is the capacitance of samples obtained from

instruments with temperature as a function of frequency. The dielectric constant and transition temperature were found to increase with increasing Bi-content in SBN. The SBN2 specimen was found to have higher value of dielectric constant as well as transition temperature compared to other two specimens SBN0 and SBN1, which is consistent with XRD, SEM and Raman data. The dielectric loss ($\tan\delta$) at room temperature has been observed 3.88×10^{-2} , 1.03×10^{-2} and 1.26×10^{-2} for SBN0, SBN1 and SBN2 respectively.

The diffusivity was found to be 1.32, 1.46 and 1.09 at 100 kHz for SBN0, SBN1, and SBN2 respectively. All three samples were found to follow the modified Curie Weiss law above the transition temperature. It was noticed that SBN0 and SBN1 show the relaxor type ferroelectric materials whereas, SBN2 is normal ferroelectric material. It has been reported in literature that SBN with the composition $\text{Sr}_{0.8}\text{Bi}_{2.2}\text{Nb}_2\text{O}_9$ have better dielectric and ferroelectric properties [10-14].

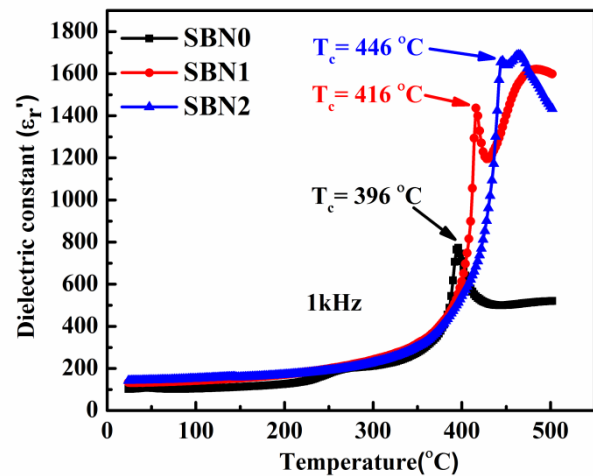


Fig. 4: Temperature of dielectric constant at 1 kHz frequency for SBN0, SBN1, and SBN2.

4. CONCLUSION

SBN ferroelectric ceramics were synthesized prepared with different Sr/Bi ratio by solid state reaction method and characterized for XRD, Raman and dielectric properties. From XRD analysis, we found single orthorhombic phase which were further analyzed for theoretical and Raman studies. A good agreement between theoretical and experimental wavenumbers was obtained. The main inferences drawn from the PED:

1. Higher wavenumbers were mainly dominated by vibrations of oxygen atoms in Nb octahedra due to their lower mass.
2. Vibrations of Bismuth atoms are mainly dominant in wavenumbers lower than 200 cm^{-1} .
3. Most of the calculated wavenumbers increases from SBN0 to SBN1 and then decreases in SBN2 which is in confirmation with experimental results.

The dielectric measurement concludes that among the studied complexes, SBN2 is the best ferroelectric material with diffusivity of 1.09 at 100 kHz.

5. ACKNOWLEDGEMENT

One of the authors (Rajveer Singh) is very thankful to Principal ARSD College, University of Delhi for granting study leave and Principal Gargi College for their support and help. The Authors R. Singh, V. Luthra and Archana thanks to Star College Grant (Department of Biotechnology) to Gargi College wide SAN/ No. 102/IFD/DBT/SAN/1911/2008-09.

REFERENCES

- [1] Araujo, C. A. P. de., Cuchiaro, J. D., McMillan, L. D., Scott, M. C., Scott, J. F., "Fatigue-free ferroelectric capacitors with platinum electrodes", *Nat.*, 374, 1995, pp. 627-629.
- [2] Desu, S. B., Vijay, D. P., "Novel fatigue-free layered structure ferroelectric thin films", *Mater. Sci. Eng. B.*, 32, 1995, pp.75-81.
- [3] Scott, J. F., Araujo, C. A. P. de, "Ferroelectric memories" *Sci.*, 246, 1989, pp. 1400-1405.
- [4] Watanabe, H., Mihara, T., Yoshimori, H., Araujo, C. A. de., "Preparation of ferroelectric thin films of bismuth layer structured compounds" *Jpn. J. Appl. Phys.*, 34, 1995, pp. 5240.
- [5] Nagata, M., Vijay, D. P., Zhang, X., Desu, S. B., "Formation and properties of SrBi₂Ta₂O₉ thin films" *Phys. Status Solidi A*, 157, 1996, pp.75-82.
- [6] Shrivastava, V., Jha, A. K., Mendiratta, R. G., "Structural distortion and phase transition studies of Aurivillius type Sr_{1-x}Pb_xBi₂Nb₂O₉ ferroelectric ceramics", *Solid State Commun.*, 133, 2004, pp. 125-129.
- [7] Aurivillius, B., "Mixed bismuth oxides with layer lattices. I. Structure type of CaCb₂Bi₂O₉", *Arkiv. Kemi.*, 1, 1949, pp. 463-480.
- [8] Gupta, H.C., Archana, Luthra, V., "Lattice vibrations of ABi₂Nb₂O₉ crystals (A= Ca, Sr, Ba)", *Vibrational Spectroscopy*, 56, 2011, pp. 235-240.
- [9] Gupta, H.C., Archana, Luthra, V., "A lattice dynamical investigation of the Raman and the infrared wavenumbers of SBT (SrBi₂Ta₂O₉)", *J. of Molecular Structure*, 984, 2010, pp. 204-208.
- [10] Singh, R., Luthra, V., Rawat, R. S., Tandon, R. P., "Structural, Dielectric and Piezoelectric properties of SrBi₂Nb₂O₉ and Sr_{0.8}Bi_{2.2}Nb₂O₉ ceramics", *Ceram. Int.*, 41, 2015, pp. 4468-4478.
- [11] Noguchi, T., Hase, T., Miyasaka, Y., "Analysis of the Dependence of ferroelectric Properties of Strontium Bismuth Tantalate (SBT) Thin Films on the Composition and Process Temperature", *Jpn. J. Appl. Phys.*, 35, 1996, pp. 4900-4904.
- [12] Miura, K., Tanaka, M., "The effect of Bi Ions Substituting at the Sr Site in SrBi₂Ta₂O₉", *Jpn. J. Appl. Phys.*, 37, 1998, pp. 2554-2558.
- [13] Shimakawa, Y., Kubo, Y., Nakagawa, Y., Kamiyama, T., Asano, H., Izumi, F., "Crystal structure and ferroelectric properties of SrBi₂Ta₂O₉ and Sr_{0.8}Bi_{2.2}Ta₂O₉", *Appl. Phys. Lett.*, 74, 1999, pp. 1904-1906.
- [14] Panda, A. B., Pathak, A., Nandagoswami, M., Pramanik, P., "Preparation and characterization of nanocrystalline Sr_{1-x}Bi_{2+y}Ta₂O₉ powders", *Mater. Sci. Eng. B.*, 97, 2003, pp. 275-282.